

# Conformational Analysis of Malonamide, *N,N'*-Dimethylmalonamide, and *N,N,N',N'*-Tetramethylmalonamide

Giovanni Sandrone, David A. Dixon,\* and Benjamin P. Hay\*

Theory, Modeling, and Simulation Group, Environmental Molecular Science Laboratory, Pacific Northwest National Laboratory, Richland, Washington 99352

Received: January 4, 1999; In Final Form: February 22, 1999

This paper reports the results of a theoretical study to identify the stable conformers of malonamide, three geometric isomers of *N,N'*-dimethylmalonamide, and *N,N,N',N'*-tetramethylmalonamide at different levels of ab initio electronic structure theory. Two stable conformations are identified for each malonamide derivative examined. Only one of these 10 structures has previously been reported. The structural parameters and relative energies of these conformations are compared at the Hartree–Fock, local density functional theory, nonlocal density functional theory, and Møller–Plesset levels of theory. The results show that significant differences in both structure and energy are obtained at the different levels of theory.

## Introduction

A previous paper has described a theoretical study of the stable conformations and the potential energy surfaces for  $C(sp^2)–C(sp^3)$  rotation in the simple aliphatic amides acetamide, **1**, propanamide, **2**, 2-methylpropanamide, **3** and **4**, and 2,2-dimethyl-propanamide, **5** (see Figure 1).<sup>1</sup> In these cases, the  $C(sp^3)$  carbon is substituted with either H or  $CH_3$  groups. The current study extends this work by examining the conformations of malonamide and its *N*-methylated derivatives, **6–10** in Scheme 1. The  $C(sp^2)–C(sp^3)$  rotational potential surface in these diamides is more complex than those found in the monoamides in that the  $C(sp^3)$  substituent is an amide group yielding two possible  $C(sp^2)–C(sp^3)$  bond rotations and, in some cases, the possibility of intramolecular hydrogen bonding.

The stable conformations of malonamides are important in understanding the chemistry of several classes of molecules including bioactive peptide analogues,<sup>3–8</sup> n,3 nylon polymers,<sup>9,10</sup> and metal ion sequestering agents.<sup>11</sup> It is the last class of compounds that provides the motivation for the current study. We have recently reported on the structural aspects of metal ion complexation by the amide oxygen donor and have elucidated the optimal orientation for coordination in terms of M–O bond length, M–O=C angle, and M–O=C–X torsion angle.<sup>12,13</sup> When two amides are connected to form a potential bidentate ligand, the connecting structure constrains the orientations of the two donor groups. Malonamide-derived ligands, in which the amide groups are connected by a methylene moiety, represent one of the simplest cases of this. Understanding how ligand architecture influences metal complex stability requires knowledge of the stable ligand conformations and their relative energies. Obtaining this information in the absence of environmental effects (e.g., solvation, crystal packing) is the first step toward this goal.

Attempts to identify preferred conformations of malonamides from X-ray crystal structure data are complicated by a propensity for the amide group to form intermolecular hydrogen bonds.<sup>5,7,8</sup> Prior theoretical studies have focused almost exclusively on the most stable geometric isomer of *N,N'*-dimethylmalonamide, **8**. The earliest calculations were performed by Stern et al. using a molecular mechanics method.<sup>2a</sup> They located

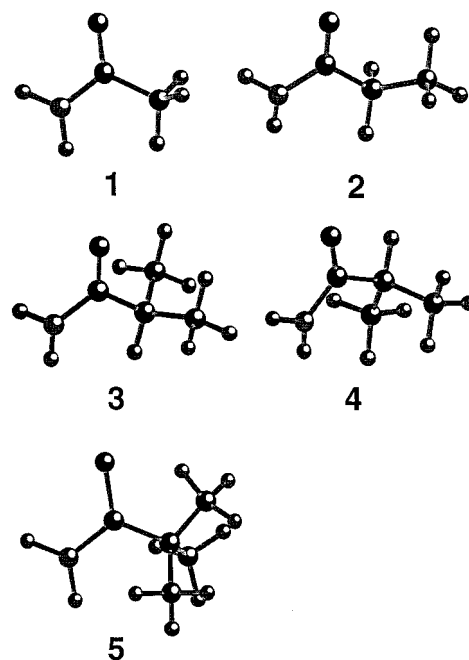
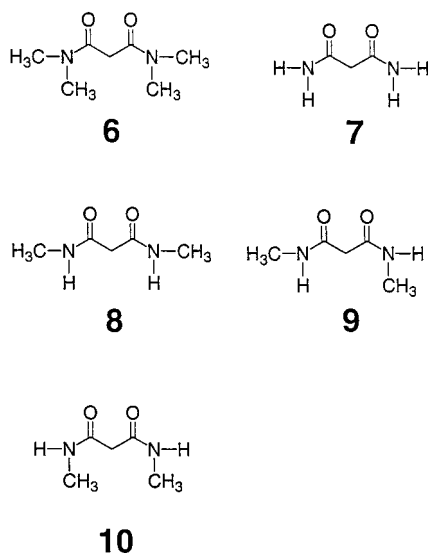


Figure 1. Simple aliphatic monoamides.

a single minimum with  $C_2$  symmetry which they later confirmed by HF/STO-3G and HF/4-31G\* calculations.<sup>2b</sup> However, full geometry optimizations were not performed. Subsequent calculations have revealed that this symmetrical minimum is not obtained when full optimizations are performed. Aleman et al. have explored the potential energy surface of **8** using the semiempirical AM1 method. Full HF/4-31G\* optimizations of the four degenerate minima yielded an asymmetric structure with an intramolecular NH–O hydrogen bond.<sup>5a,b</sup> The conformational preferences of **8** have also been explored by force field methods.<sup>5c</sup> No other stable conformations for **8** have been reported. Analogous conformations were obtained in studies of *N,N,N'*-trimethylmalonamide,<sup>3</sup> 2-methyl-*N,N'*-dimethylmalonamide,<sup>4,6</sup> and 2,2-dimethyl-*N,N'*-dimethylmalonamide.<sup>6</sup> No conformational analyses have been reported for **6**, although there has

## SCHEME 1



been a recent study of asymmetrically substituted *N,N,N',N'*-tetraalkylmalonamides.<sup>11</sup> No conformational analyses have been reported for **7**.

Herein we report the results of a theoretical study to identify the stable conformers of **6–10** at different levels of ab initio electronic structure theory with correlation effects included. We have adopted the following strategy to avoid exhaustive dihedral angle scans for each molecule. First we examined the potential energy surface of **6** in which no intramolecular  $\text{NH}\cdots\text{O}$  hydrogen bonding can occur. This yielded two conformers. Then we examined **7** for all possible structures in which intramolecular hydrogen bonding could occur. This yielded two other conformers. Conformations obtained with **6** and **7** provided the starting points for **8**, **9**, and **10**. The structural parameters and relative energies for these conformers are presented. The results demonstrate that significant differences in both structure and energy are obtained at different levels of theory.

## Methods

The calculations were done at both the ab initio molecular orbital (MO) theory and density functional theory (DFT) levels. The DFT calculations were done with the program system DGauss.<sup>14</sup> The DFT calculations were done with the DZVP2 basis set and the A1 fitting basis set.<sup>15</sup> Calculations were done at the local level (LDFT) with the Vosko, Wilk, and Nusair fit of the correlation energy and Slater exchange<sup>16</sup> and at the gradient-corrected (nonlocal) level (NLDF) with the Becke exchange functional<sup>17</sup> and the Perdew correlation functional.<sup>18</sup> The MO calculations were done at the Hartree–Fock (HF) and Møller–Plesset (MP2) levels with the programs GAUSSIAN94<sup>19</sup> and NWCHEM.<sup>20</sup> The MO calculations were done with a polarized double- $\zeta$  basis set.<sup>21</sup> Geometries were optimized at all levels for the different conformers. Frequencies were calculated analytically for all conformers at all levels except for **6** at the MP2 level. Final energy calculations were done at the appropriate optimized geometry with larger basis sets, TZVP for the DFT calculations<sup>15</sup> and aug-cc-pVDZ and aug-cc-pVTZ for the MO calculations.<sup>22,23</sup>

## Results and Discussion

*N,N,N',N'*-Tetramethylmalonamide (**6**). A potential energy surface for rotation about one of the C–C bonds in *N,N,N',N'*-tetramethylmalonamide was calculated at the MP2/DZP level

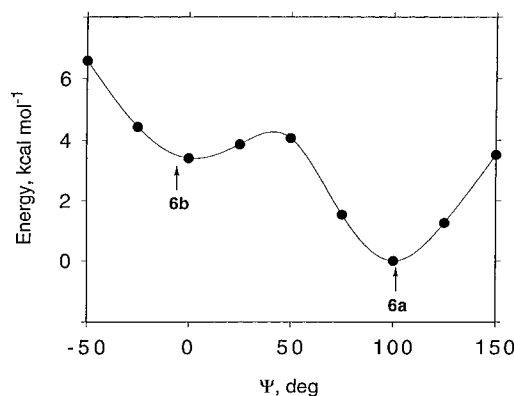


**Figure 2.** Plot of relative energy (MP2/DZP) versus  $\Psi$  (the  $\text{C}_3\text{--C}_5\text{--C}_6\text{=O}_7$  dihedral) yielding a potential energy surface for rotation about the  $\text{C}_5\text{--C}_6$  bond in **6**.

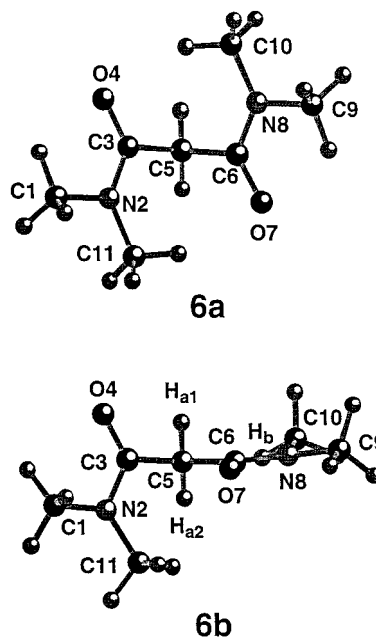


**Figure 3.** Optimized MP2/DZP geometries of **6**.

(see Figure 2). The nine different conformers on this rotational potential energy curve were optimized by freezing the value of  $\Psi$ , the  $\text{C}_3\text{--C}_5\text{--C}_6\text{=O}_7$  dihedral angle ( $\Psi = -50^\circ, -25^\circ, 0^\circ, 25^\circ, 50^\circ, 75^\circ, 100^\circ, 125^\circ, \text{ and } 150^\circ$ ). Two stable conformers, **6a** and **6b**, were obtained by full optimization of the structures at  $\Psi = 100^\circ$  and  $\Psi_1 = 25^\circ$ . These conformers are shown Figure 3. Structural parameters at all levels of theory are reported in Table 1. Relative energies at all levels of theory are reported in Table 2.

The lowest energy conformer, **6a**, occurs at  $\Psi = 108.8^\circ$  and has  $\text{C}_2$  symmetry. In this conformer, the two  $\text{C=O}$  dipoles are oriented in opposite directions, minimizing unfavorable dipole–dipole interactions. In addition, there are close contacts (2.26 Å) between the oxygen of one amide and a methyl hydrogen of the other amide. These close contacts suggest the presence of further stabilization through two  $\text{O}\cdots\text{H}(\text{CH}_2)$  hydrogen bonds. Analogous  $\text{O}\cdots\text{H}\text{--C}$  hydrogen bonding interactions are often observed in cases when the acceptor oxygen occurs in water, an alcohol, or an ether.<sup>24</sup>

The second conformer, **6b**, occurs at  $\Psi = 10.8^\circ$ . This conformer is higher in energy than **6a** at all levels of theory (see Table 2). At our best level of theory, MP2/DZP//MP2/cc-aug-pVTZ, the energy difference is 2.84 kcal mol<sup>-1</sup>. The higher energy of **6b** can be attributed to both the less favorable

**TABLE 1: Calculated Geometry of 6a and 6b<sup>a</sup>**

parameter	HF		LDFT		NLDFT		MP2	
	6a	6b	6a	6b	6a	6b	6a	6b
C3–O4	1.211	1.206	1.245	1.239	1.251	1.245	1.246	1.241
C6–O7	1.211	1.205	1.245	1.239	1.251	1.246	1.246	1.241
C3–N2	1.351	1.360	1.356	1.364	1.375	1.383	1.368	1.375
C6–N8	1.351	1.359	1.356	1.360	1.375	1.379	1.368	1.375
C1–N2	1.453	1.455	1.440	1.441	1.466	1.467	1.457	1.458
C11–N2	1.455	1.452	1.444	1.440	1.468	1.465	1.459	1.456
C10–N8	1.455	1.451	1.444	1.440	1.468	1.465	1.459	1.456
C9–N8	1.453	1.454	1.440	1.442	1.466	1.468	1.457	1.458
C6–C5	1.531	1.525	1.516	1.516	1.542	1.540	1.531	1.531
C3–C5	1.531	1.525	1.516	1.513	1.542	1.537	1.531	1.525
C2–C5–C6	113.0	111.6	112.9	112.1	114.5	112.7	112.1	110.9
C10–N8–C9	115.1	115.5	116.8	116.8	115.8	115.8	115.5	115.7
C1–N2–C11	115.1	114.6	116.8	115.8	115.7	115.1	115.5	114.7
O7–C6–N8	122.7	122.6	122.5	122.1	122.4	122.2	122.6	122.5
O4–C3–N2	122.7	122.5	122.5	122.5	122.4	122.4	122.6	122.7
O7–C6–C5	118.6	120.4	120.4	121.6	119.7	121.5	119.9	121.3
O4–C3–C5	118.6	118.2	120.4	119.5	122.4	122.4	122.6	122.7
C9–N8–C6	119.1	118.5	118.5	118.3	118.6	118.5	118.9	118.9
C10–N8–C6	125.2	123.8	124.6	124.2	124.8	123.9	125.4	123.9
C11–N2–C3	125.2	123.5	124.5	123.7	124.9	123.8	125.4	123.9
C1–N2–C3	115.1	117	118.5	117.3	118.6	117.3	118.9	117.5
C9–N8–C6–O7	4.5	8.3	4.1	6.9	4.7	7.6	3.9	7.0
C10–N8–C6–O7	175.5	169.5	179.8	173.9	174.6	171.5	177.6	172.8
C9–N8–C6–C5	-175.5	-173.4	-176.1	-174.0	-175.2	-173.6	-176.9	-174.1
C10–N8–C6–C5	-4.6	-12.3	-0.4	-7.0	-5.2	-9.7	-3.2	-8.4
C11–N2–C3–O4	175.5	162.6	-179.8	169.4	174.2	165.2	177.4	164.7
C1–N2–C3–O4	4.5	8.2	4.5	8.8	4.9	7.8	4.0	8.4
C11–N2–C3–C5	-4.6	-21.7	0.0	-13.0	-5.8	-18.7	-3.4	-18.3
C1–N2–C3–C5	-175.5	-176.2	-175.7	-173.7	-175.2	-176.1	-176.8	-174.6
N8–C6–C5–C3	-81.1	170.5	-77.4	167.4	-77.4	170.3	-78.5	170.5
N2–C3–C5–C6	-81.1	84.9	-77.9	75.6	-77.1	81.9	-78.4	81.2
O7–C6–C5–C3	98.9	-11.2	102.4	-13.5	102.7	-10.8	100.8	-10.7
O4–C3–C5–C6	98.9	-99.2	101.9	-106.8	102.9	-101.9	100.8	-101.8

<sup>a</sup> Bond distances in Å. Angles in degrees.**TABLE 2: Relative Stabilities of Conformer Pairs for 6–10<sup>a</sup>**

	HF			LDFT		NLDFT		MP2		
	DZP	pVDZ	pVTZ	DZVP2	TZVP	DZVP2	TZVP	DZP	pVDZ	pVTZ
<b>6b–6a</b>	1.20	0.88	1.40	5.98	5.01	3.96	3.41	3.14	2.63	2.84
<b>7b–7a</b>	4.65	4.45	4.47	6.26	6.20	4.83	4.77	4.19	3.97	4.22
<b>8b–8a</b>				7.10	7.04	5.54	5.53	4.54	4.10	4.37
<b>9a–8a</b>	3.26	3.27	3.41	3.89	6.67	3.43	3.73	2.47	2.23	1.71
<b>9b–9a</b>								3.78	3.34	3.57
<b>10a–8a</b>	7.47	7.44	7.74	6.75	7.21	6.74	7.28	5.81	5.20	4.93
<b>10b–10a</b>	1.53	0.88	1.40	4.93	2.93	3.61	4.77	2.83	2.69	2.97

<sup>a</sup>  $\Delta E$  values (kcal/mol). DZP = polarized double- $\zeta$  basis set, pVDZ = aug-cc-pVDZ, pVTZ = aug-cc-pVTZ.**TABLE 3: Close Hydrogen Contacts along the C–C Rotational Surface in 6<sup>a</sup>**

$\Psi$	H <sub>b</sub> –H <sub>a1</sub>	H <sub>b</sub> –H <sub>a2</sub>
-25.0°	2.581	2.018
0.0°	2.364	2.166
10.7° (min)	2.304	2.265
25.0°	2.063	2.469

<sup>a</sup> See Figure 3 for hydrogen assignments.

orientation of the C=O dipoles and the loss of the stabilizing O···H(CH<sub>2</sub>) hydrogen bonds. The **6b** conformer is stabilized by a minimization of the steric interactions between the methyl hydrogen, H<sub>b</sub>, and the methylene hydrogens, H<sub>a1</sub> and H<sub>a2</sub> (see Figure 3). Table 3 reports the values of the distances H<sub>b</sub>–H<sub>a1</sub> and H<sub>b</sub>–H<sub>a2</sub> as a function of  $\Psi$ . On either side of the minimum one of the two possible H<sub>a</sub>–H<sub>b</sub> distances becomes quite short; H<sub>a1</sub>–H<sub>b</sub> is 2.063 Å at  $\Psi = 25^\circ$  and H<sub>a2</sub>–H<sub>b</sub> is 2.018 Å at  $\Psi_1 = -25^\circ$ . These severe steric clashes are minimized at  $\Psi = 10.8^\circ$  where the H<sub>a</sub>–H<sub>b</sub> distances are 2.265 and 2.304 Å.

**Malonamide (7).** Intramolecular hydrogen bonding results in conformations for **7** that differ substantially from those located for **6**. The two stable conformations of malonamide (**7a** and **7b**) are shown in Figure 4. If calculations are performed on **7** using initial geometries corresponding to either **6a** or **6b**, then **7a** is obtained. Structural parameters at all levels of theory are reported in Table 4. Relative energies at all levels of theory are reported in Table 2.

The more stable of the two structures, **7a**, has a NH···O hydrogen bond. This interaction involves the hydrogen that is trans to the carbonyl group which has been found to be a stronger hydrogen bond donor than the hydrogen cis to the carbonyl group.<sup>25</sup> The H···O distance is 2.135 Å at the HF level, 1.824 Å at the LDFT level, 2.036 Å at the NLDFT level, and 2.086 Å at the MP2 level. The H···O distance at the MP2 level is comparable to the value of 2.076 Å calculated for the *trans*-N-methylacetamide dimer (MP2/DZP).<sup>26</sup> Our H···O distances correspond to heavy atom N···O distances of 2.855 Å, 2.685, 2.838, and 2.849 Å for the HF, LDFT, NLDFT, and MP2 levels

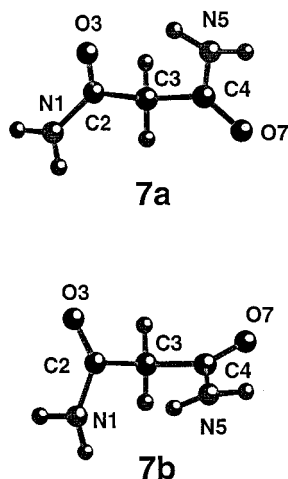


Figure 4. Optimized MP2/DZP geometries of 7.

of theory, respectively. The C=O bond of the hydrogen bond acceptor is longer, by 0.003 to 0.009 Å, than the other C=O bond at all levels of theory. The C–N bond of the hydrogen bond donor is less noticeably affected with changes ranging from –0.001 to 0.004 Å, depending on the level of theory.

The less stable of the two structures, **7b**, has a NH···N hydrogen bond. This hydrogen bond also involves the hydrogen that is trans to the carbonyl group. The H···N distance is 2.562 Å at the HF level, 2.224 Å at the LDFT level, 2.439 Å at the NLDFT level, and 2.323 Å at the MP2 level. These distances correspond to heavy atom N···N distances of 3.20 Å, 2.94, 3.16, and 3.05 Å for the HF, LDFT, NLDFT, and MP2 levels of theory, respectively. The intramolecular NH···N distance at the HF level is significantly shorter than the intermolecular NH···N value of 3.54 Å calculated for the acetamide dimer (HF/6-31G\*\*).<sup>25</sup> The C–N bond length of the hydrogen bond acceptor is significantly longer, by 0.013 to 0.023 Å, than the C–N bond length of the hydrogen bond donor at all levels of theory. The C=O bond distances, however, are less noticeably affected with changes of only 0.001 to 0.002 Å.

At the HF/DZP level, **7a** is 4.6 kcal mol<sup>–1</sup> more stable than **7b**.  $\Delta E$  slightly decreases (4.5 kcal mol<sup>–1</sup>) as the quality of the basis set is improved (aug-cc-pVDZ, aug-cc-pVTZ). The MP2

method predicts a slightly smaller energy difference of 4.2 kcal mol<sup>–1</sup> with the DZP basis set. The value decreases to 4.0 kcal mol<sup>–1</sup> with the aug-cc-pVDZ basis set. We also calculated the energy difference with the aug-cc-pVDZ basis set and the energy only changed by a small amount to 4.2 kcal mol<sup>–1</sup>. The DFT calculations also predict **7a** to be the most stable conformer. The NLDFT values are 4.8 kcal mol<sup>–1</sup> with both the double- and triple- $\zeta$  basis sets, similar to the HF values and about 0.6–0.8 kcal mol<sup>–1</sup> above the MP2 values. The LDFT value for DE is 6.3 kcal mol<sup>–1</sup> with the DZVP2 basis sets and 0.1 kcal mol<sup>–1</sup> higher when TZVP is adopted.

The stability of **7a** over **7b** can be attributed to two main factors. First, as in **6a**, unfavorable C=O dipole–dipole interactions are minimized in **7a** relative to **7b**. Second, studies of the intermolecular interactions between two amides reveal that the strength of the NH···O hydrogen bond (6–7 kcal mol<sup>–1</sup>) is stronger than that of the NH···N hydrogen bond (1–2 kcal mol<sup>–1</sup>).<sup>25–27</sup> In the specific case of acetamide dimers, in which the hydrogen bond donor is the trans hydrogen, the difference between a NH···O hydrogen bond and a NH···N hydrogen bond is 5.0 kcal mol<sup>–1</sup>.<sup>25</sup> This difference is comparable to the energy differences obtained between **7a** and **7b** (see Table 2).

***N,N'*-Dimethylmalonamide (8, 9, and 10)**. We now turn our attention to the case where each nitrogen is substituted with one methyl group and one hydrogen. Because the barrier to rotation about the amide bond (N–C(=O)) is large, on the order of 16–20 kcal mol<sup>–1</sup>,<sup>28</sup> *N,N'*-dimethylmalonamide exhibits three geometric isomers. The orientation, cis or trans, of the methyl groups relative to the carbonyl groups distinguishes these isomers. Using this designation, the three cases are the cis–cis form, **8**, the cis–trans form, **9**, and the trans–trans form, **10**.

***Cis-cis Form (8)***. The two stable conformations of the cis–cis form (**8a** and **8b**) are shown in Figure 5. Dihedral angles at all levels of theory are reported in Table 5. Relative energies at all levels of theory are reported in Table 2. These conformations are similar to those observed for **7**. Attempts to locate additional stable conformations using initial geometries corresponding to **6a** and **6b** yielded **8a** at all levels of theory.

The more stable conformer, **8a**, with a NH···O hydrogen bond, corresponds to **7a**. The hydrogen bonded ring structure in **8a** shows an O···H distance of 2.129 Å at the HF level, with

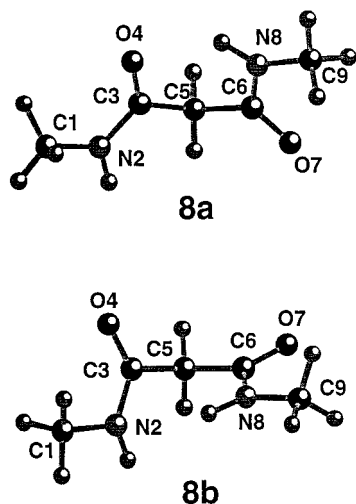
TABLE 4: Calculated Geometry of **7a** and **7b**<sup>a</sup>

parameter	HF		LDFT		NLDFT		MP2	
	<b>7a</b>	<b>7b</b>	<b>7a</b>	<b>7b</b>	<b>7a</b>	<b>7b</b>	<b>7a</b>	<b>7b</b>
C2–O6	1.206	1.198	1.242	1.228	1.247	1.236	1.240	1.231
C4–O7	1.203	1.200	1.233	1.23	1.240	1.237	1.235	1.232
C2–N1	1.350	1.368	1.354	1.379	1.371	1.396	1.367	1.394
C4–N5	1.350	1.356	1.350	1.357	1.370	1.375	1.368	1.371
C3–C2	1.520	1.519	1.506	1.506	1.530	1.529	1.523	1.520
C3–C4	1.528	1.528	1.527	1.524	1.547	1.550	1.534	1.537
C2–C3–C4	115.1	115.7	114.9	117.1	115.0	115.7	112.9	114.2
N1–C2–O6	122.2	122.0	125.6	121.5	121.8	121.6	122.3	121.9
N5–C4–O7	123.7	122.6	125.4	123.1	124.5	123.0	124.1	123.1
H10–N1–H11	119.3	117.2	120.2	117.7	119.4	116.2	119.3	115.5
H13–N5–H12	119.8	118.8	122.8	121.3	119.9	119.3	119.6	119.5
O6–C2–C3	122.1	122.1	122.6	123.1	121.8	122.8	122.4	123.2
O7–C4–C3	120.0	119.9	120.5	120.2	120.9	120.7	121.5	121.2
N1–C2–C3–C4	128.4	–86.9	134.6	–67.8	130.5	–83.7	122.5	–82.5
N5–C4–C3–C2	47.4	27.3	38.8	14.6	47.7	33.6	52.0	35.0
O6–C2–C3–C4	–53.5	90.1	–46.6	108.7	–50.8	91.9	–58.5	92.5
O7–C4–C3–C2	–135.9	–155.9	–143.7	–166.3	–136.0	–149.9	–131.0	–148.0
H10–N1–C2–O6	2.2	11.4	1.5	12.2	2.5	13.4	4.3	14.6
H11–N1–C2–O6	175.2	162.6	176.0	161.1	174.9	157.9	172.9	155.7
H12–N5–C4–O7	167.0	171.5	168.6	179.6	164.5	170.2	164.4	171.4
H13–N5–C4–O7	7.9	7.6	8.1	2.2	11.6	9.0	10.5	7.7

<sup>a</sup> Bond distances in Å. Angles in degrees.

TABLE 5: Dihedral Angles (degrees) for **8a** and **8b**

parameter	HF	LDFT		NLDFT		MP2	
	<b>8a</b>	<b>8a</b>	<b>8b</b>	<b>8a</b>	<b>8b</b>	<b>8a</b>	<b>8b</b>
O4–C3–C5–C6	57.4	39.2	90.6	53.2	87.9	60.0	90.2
O7–C6–C5–C3	136.1	155.5	–152.5	144.7	–148.4	134.1	–150.4
N8–C6–C5–C3	–124.1	–26.5	29.1	–37.5	34.0	–48.4	31.8
N2–C3–C5–C6	–46.7	–142.0	–85.3	–127.3	–88.4	–120.6	–85.4
C9–N8–C5–C6	178.2	–177.6	–178.1	–179.1	–177.8	177.8	–179.0
C1–N2–C3–C5	179.5	178.2	–176.9	–178.9	–176.8	178.4	–174.1
C9–N8–C6–O7	–4.7	0.2	3.5	–1.5	4.7	–4.8	3.2
C1–N2–C3–O4	–2.0	0.7	7.1	0.6	6.9	–2.3	10.3

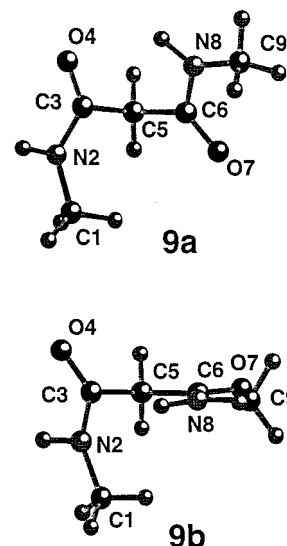
Figure 5. Optimized MP2/DZP geometries of **8**.

shorter values predicted at the DFT levels (1.790 and 1.999 Å at LDFT and NLDFT, respectively) or at the MP2 level (2.054 Å). These distances are quite similar to those found in malonamide **7a**.

The other conformer, **8b**, with a NH···N hydrogen bond, corresponds to **7b**. All of our attempts to locate structure **8b** at the HF level failed as any optimization without symmetry always found structure **8a**. However, the DFT and MP2 methods do predict the existence of a minimum energy structure **8b** in which the distance between the two nitrogen atoms (3.10 Å, MP2) is larger than that in **7b** (3.05 Å, MP2). The presence of the NH···N hydrogen bond in **8b** gives rise to differences in the N8–C6 and N2–C3 bond distances, as previously noticed in **7b**. The reduction of the N8–C6 bond distance and the elongation of the N2–C3 bond distance lead to a difference of 0.02 Å at the MP2 level.

In a prior study, Aleman and Perez explored the potential energy surface of the cis–cis isomer of **8** using the AM1 semiempirical method and then tested the results at the HF/3-21G and HF/4-31G\* levels.<sup>5</sup> A single conformer, equivalent to **8a**, was located with this approach. This structure exhibits C–C–C–N dihedral angles of 52° and 111°, in comparison to our HF values of 47° and 124°. The C<sub>2</sub> conformer obtained by Stern et al.<sup>2</sup> using force field methods (similar to **6a**) is not a minimum at any level of theory examined in this study.

*Cis–trans Form (9)*. The two stable conformations of the cis–trans form (**9a** and **9b**) are shown in Figure 6. Dihedral angles at all levels of theory are reported in Table 6. Relative energies at all levels of theory are reported in Table 2. The stable conformations of **9** are similar to those observed for **7** and **8**. Attempts to locate additional stable conformations using initial geometries corresponding to **6a** and **6b** yielded **9a** at all levels of theory.

Figure 6. Optimized MP2/DZP geometries of **9**.TABLE 6: Dihedral Angles (deg) for **9a** and **9b**

parameter	HF	LDFT	NLDFT	MP2	
	<b>9a</b>	<b>9a</b>	<b>9a</b>	<b>9a</b>	<b>9b</b>
O4–C3–C5–C6	122.0	132.1	121.8	117.8	107.4
O7–C6–C5–C3	78.7	69.2	81.5	85.2	–173.3
N8–C6–C5–C3	–50.1	–50.1	–59.2	–62.4	6.1
N2–C3–C5–C6	–100.1	–110.0	–96.2	–91.6	–68.7
C9–N8–C5–C6	175.9	176.8	175.5	174.2	–178.5
C1–N2–C3–C5	2.2	1.5	2.5	0.8	–24.5
C9–N8–C6–O7	–5.6	–5.6	–5.5	–5.9	0.9
C1–N2–C3–O4	–176.6	177.6	–175.1	–176.2	159.4

The more stable conformer, **9a**, with a NH···O hydrogen bond corresponds to **7a**. The H···O distance is 2.345 Å at the HF level, 2.117 Å at the LDFT level, 2.350 Å at the NLDFT level, and 2.357 Å at the MP2 level. These distances are significantly longer than those found in **7a** or **8a**, suggesting a weaker NH···O hydrogen bond in the case of **9a**. At our highest level of theory, **9a** is 1.7 kcal mol<sup>–1</sup> less stable than **8a** (see Table 2). This energy difference is anticipated as a 1–3 kcal mol<sup>–1</sup> preference for methyl orientation cis to the carbonyl group is well-known in monoamides.<sup>26,28,29</sup> For example, the cis and trans isomers of *N*-methylacetamide differ in energy by 2.3 kcal mol<sup>–1</sup>.<sup>26</sup>

The other conformer, **9b**, with a NH···N hydrogen bond corresponds to **7b**. This structure is found to be a real minimum on the potential energy surface only at the MP2 level as the Hartree–Fock and DFT methods are only able to find a minimum energy structure for **9a**. The distance between the two nitrogen atoms (3.03 Å) is slightly shorter than that obtained with **7b** (3.05 Å). As before, the presence of the NH···N hydrogen bond in **9b** gives rise to differences in the N8–C6 and N2–C3 bond distances as previously noticed in **7b**.

TABLE 7: Dihedral Angles (Degrees) for 10a and 10b

parameter	HF		LDFT		NLDFT		MP2	
	10a	10b	10a	10b	10a	10b	10a	10b
O4-C3-C5-C6	93.4	97.9	98.5	105.7	96.6	101.6	98.8	101.4
O7-C6-C5-C3	93.5	17.3	98.5	16.4	96.6	16.6	98.8	12.7
N8-C6-C5-C3	-85.9	-164.9	-79.8	-164.6	-82.7	-164.8	-79.2	-169.3
N2-C3-C5-C6	-86.0	-85.9	-79.8	-76.9	-82.7	-81.8	-79.2	-82.0
C9-N8-C5-C6	-3.9	11.2	-4.5	6.0	-5.1	9.0	-8.3	12.6
C1-N2-C3-C5	-3.9	20.9	-4.0	14.8	-4.9	17.9	-8.3	21.2
C9-N8-C6-O7	176.7	-171.0	177.7	-175.0	175.7	-172.3	173.7	-169.4
C1-N2-C3-O4	176.7	-163.0	177.7	-167.8	173.8	-165.6	173.7	-162.3

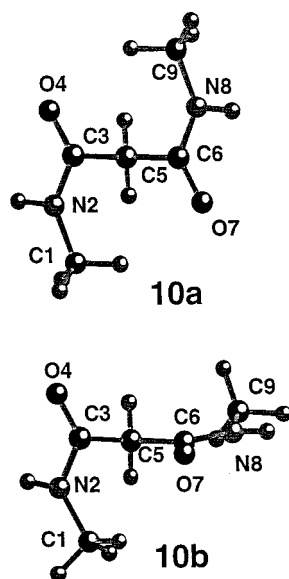


Figure 7. Optimized MP2/DZP geometries of 10.

*Trans-trans form (10).* The two stable conformations of the trans-trans form (**10a** and **10b**) are shown in Figure 7. Dihedral angles at all levels of theory are reported in Table 7. Relative energies at all levels of theory are reported in Table 2. With both *N*-methyl substituents oriented trans to the carbonyl groups, **10** cannot form intramolecular hydrogen bonds and the stable conformations are analogous to those observed for **6**. At our best level of theory, **10a** is 4.9 kcal mol<sup>-1</sup> above **8a**, which is again consistent with the expected magnitude of the energy difference for converting two cis methyl groups into two trans methyl groups.

**Vibrational Frequencies.** Vibrational frequencies were calculated to establish the absence of any negative modes, i.e., to verify that all structures reported here represent true minima on the potential energy surface. The low-frequency ( $\leq 100$  cm<sup>-1</sup>) modes for all the structures are given in Table 8. The two lowest frequency modes for all of the compounds correspond to torsion about the C-C bonds. Also of interest are the carbonyl stretching frequencies, as these modes give rise to the strong absorptions in vibrational spectra that are potentially of use in structural assignments. The carbonyl stretching frequencies for all the structures, also presented in Table 8, are discussed below.

We take the frequencies for **6a** to represent those for the carbonyl in a non-hydrogen bonded environment. The carbonyl frequencies show only a small splitting between the symmetric and the asymmetric coupling of the C=O stretches. The asymmetric coupling has a large infrared intensity and the symmetric coupling a low infrared intensity consistent with the orientations of the carbonyl groups. As expected, the magnitudes of the frequencies are in the order HF > LDFT > NLDFT.<sup>30</sup> The frequencies and the splitting between the two modes

TABLE 8: Lowest Frequencies and C=O Stretching Frequencies (cm<sup>-1</sup>) for All Conformers Analyzed in the Present Study<sup>c</sup>

conformer	HF	LDFT	NLDFT	MP2
<b>6a</b>	24	47	32	<i>a</i>
	54	75	65	<i>a</i>
	1887 a (1064)	1705 a (775)	1655 a (752)	<i>a</i>
<b>6b</b>	1889 s (0.02)	1706 s (22)	1661 s (11)	<i>a</i>
	37	43.3	30.9	<i>a</i>
	69	75.8	61.3	<i>a</i>
<b>7a</b>	1909 a (515)	1720 a (354)	1673 a (387)	<i>a</i>
	1923 s (426)	1730 s (380)	1681 s (305)	<i>a</i>
	44	63	40	48
<b>7b</b>	54	84	71	74
	1938 (350)	1736 (247)	1701 (271)	1796 (250)
	1957 (685)	1784 (513)	1732 a (477)	1801 (374)
<b>8a</b>	23	50	32	52
	37	75	62	61
	1962 a (570)	1770 a (474)	1728 a (351)	1783 a (209)
<b>8b</b>	1983 s (456)	1783 s (313)	1737 s (403)	1800 s (459)
	32	17	43	36
	43	72	64	43
<b>9a</b>	1911 (223)	1711 (183)	1671 (165)	1752 (140)
	1933 (602)	1762 (450)	1710 (450)	1778 (416)
	<i>b</i>	39	38	31
<b>9b</b>	<i>b</i>	60	56	55
	<i>b</i>	1752 a (289)	1706 a (257)	1773 a (226)
	<i>b</i>	1764 s (338)	1719 s (368)	1780 s (299)
<b>10a</b>	30	50	21	44
	43	72	47	49
	93	132	55	62
<b>10b</b>	1918 (460)	1720 (297)	1683 (368)	1765 (132)
	1936 (528)	1762 (442)	1706 (345)	1774 (525)
	<i>b</i>	<i>b</i>	<i>b</i>	28
<b>10a</b>	<i>b</i>	<i>b</i>	<i>b</i>	61
	<i>b</i>	<i>b</i>	<i>b</i>	67
	<i>b</i>	<i>b</i>	<i>b</i>	1767 (347)
<b>10b</b>	<i>b</i>	<i>b</i>	<i>b</i>	1778 (279)
	30	46	45	40
	99	105	109	113
<b>10a</b>	1922 a (1184)	1740 a (855)	1689 a (851)	1767 s (0.1)
	1926 s (15.6)	1742 s (35)	1695 s (1.4)	1768 a (797)
	31	13	21	35
<b>10b</b>	66	48	72	84
	1936 a (618)	1749 a (420)	1699 a (451)	1775 a (401)
	1952 s (486)	1759 s (420)	1709 s (341)	1783 s (325)

<sup>a</sup> Structure was located but frequency calculations were computationally too expensive to perform. <sup>b</sup> Structure was not located at this level of theory. <sup>c</sup> Data in parentheses are the intensities of the C=O stretching modes in km mol<sup>-1</sup>.

increase for the less stable conformer **6b**, and the intensities for both couplings are large.

For **7a**, the frequencies are blue shifted from those in **6a**. The lower C=O frequency occurs with the H-bonded carbonyl and the higher frequency occurs with the non-hydrogen-bonded carbonyl. The largest difference in the frequencies is at the LDFT level, consistent with the exaggeration of the H-bond strength at this level. The MP2 frequencies show only a small

splitting for **7a**. The frequencies for **7b** do not show much change from those in magnitude as compared to **7a**, except that there is a slight increase in the splitting at the MP2 level. The assignments for **7b** are now in terms of the symmetric and asymmetric coupling of the C=O stretches. In contrast to the results for **6a**, both modes in **7a** show significant infrared intensities.

For **8a**, there is a significant splitting of the two modes even at the MP2 level with a smaller splitting predicted for **8b**. Both modes are predicted to have significant intensities. For **8a**, the lower frequency mode is predicted to be that for the H-bonded carbonyl group. For **9a** and **9b**, the splitting is smaller and both modes still have significant intensity. Again, the H-bonded carbonyl has the lower frequency. For **10a** and **10b**, the modes exhibit behavior similar to that of **6a** and **6b**, as expected because no hydrogen bonds can be formed to the carbonyl groups. The modes in **10a** are slightly blue-shifted as compared to those in **6b**, showing the effect of the additional methyl substitution on the nitrogen.

## Discussion

Malonamide and *N*-methylated malonamide derivatives can adopt several stable conformations in the gas phase. When intramolecular hydrogen bonding is not possible, as in **6** and **10**, two conformers are observed. The lowest energy conformations, **6a** and **10a**, in which the two carbonyl groups are oriented in opposite directions, are stabilized by minimization of intramolecular dipole–dipole interactions. In addition, the close contacts between the oxygens and *N*-methyl hydrogens suggest additional stabilization from O $\cdots$ H(CH<sub>3</sub>) hydrogen bonding. On rotation about one of the C–C bonds, higher energy conformations **6b** and **10b** are stabilized as one of the hydrogens of the *N*-methyl group meshes with the two hydrogens of the central methylene.

Intramolecular hydrogen bonds can form when a nitrogen bears a hydrogen trans to the carbonyl group as in **7**, **8**, and **9**. Neither of the two conformations of **6** and **10** are observed when intramolecular hydrogen bonding is possible. Here, the most stable conformations, **7a**, **8a**, and **9a**, all contain an intramolecular NH $\cdots$ O hydrogen bond. A higher energy conformation observed in **7b**, **8b**, and **9b** is stabilized by an intramolecular NH $\cdots$ N hydrogen bond. These conformations can be viewed as distorted versions of the C<sub>2</sub> conformation observed in **6a** and **10a**, i.e., if the intramolecular hydrogen bonding were turned off, then C<sub>2</sub> conformations would be obtained. This may be the case in condensed phases where hydrogen bonding would be weakened by the increased dielectric and by specific solvent interactions.<sup>5–7</sup>

Comparison of the structures and energies at various levels of theory reveals some expected trends. The HF bond lengths are all shorter and the HF frequencies are higher than those obtained with the correlated methods.<sup>30</sup> The short hydrogen bonds obtained at the LDFT level are consistent with the results of other calculations that reveal the LDFT level exaggerates the hydrogen bond energies.<sup>31</sup> The HF method fails to locate two of the minima, **8b** and **9b**. This may be a result of the known tendency for HF to underestimate hydrogen bond strengths,<sup>32</sup> i.e., an underestimation of the NH $\cdots$ N interaction needed to stabilize these conformations. Although both DFT methods locate **8b**, they fail to locate **9b**. The reason for this failure is not obvious.

With respect to the relative energies, it is not possible to judge the performance of the various levels of theory against experiment because such data is not available for **6–10**. We can,

however, compare the relative energies at other levels of theory to those obtained our best level of theory, the MP2/DZP//MP2/aug-cc-pVTZ level. In all cases where comparisons are possible, all levels of theory give the same qualitative ordering of conformer stability. Quantitatively, however, there are significant differences in relative energies. In the absence of hydrogen bonding (**6b–6a** and **10b–10a**), HF underestimates the energy differences by an average of 1.5 kcal mol<sup>-1</sup>, LDFT underestimates one and overestimates the other with an average discrepancy of 1.1 kcal mol<sup>-1</sup>, and NLDFT overestimates both by an average of 1.8 kcal mol<sup>-1</sup>. When hydrogen bonding is present (**7b–7a** and **8b–8a**), HF overestimates the energy difference by 0.3 kcal mol<sup>-1</sup>, LDFT overestimates both by an average of 3.4 kcal mol<sup>-1</sup>, and NLDFT overestimates both by an average of 0.9 kcal mol<sup>-1</sup>.

The results obtained in the current study, as well as those obtained in our prior study of simple aliphatic amides,<sup>1</sup> show significant differences in the energies of amide conformations at the different levels of theory. The results reveal that, with this class of molecules, using the computationally less expensive HF and DFT methods does not yield the same quantitative result as the more costly, and presumably more accurate, MP2 method. In support of the MP2 results, force field parameters (MM3) fit to the MP2/DZP potential energy surface shown in Figure 2 and to MP2/DZP potential energy surfaces for C(sp<sup>2</sup>)–C(sp<sup>3</sup>) rotations in monoamides yield a molecular mechanics model that reproduces the experimentally observed conformations of amides<sup>1</sup> and their metal complexes.<sup>13</sup>

**Acknowledgment.** This work was supported by the Environmental Management Science Program under direction of the U.S. Department of Energy's Office of Basic Energy Sciences (ER-14), Office of Energy Research and the Office of Science and Technology (EM-52), Office of Environmental Management. The research described in this manuscript was performed at the W. R. Wiley Environmental Molecular Sciences Laboratory (EMSL), a national scientific user facility sponsored by the U.S. Department of Energy's Office of Biological and Environmental Research and located at Pacific Northwest National Laboratory. Pacific Northwest National Laboratory is operated for the Department of Energy by Battelle. Some of the calculations were performed on the IBM SP computer in the Molecular Science Computing Facility of the EMSL.

**Supporting Information Available:** Cartesian coordinates of optimized structures in angstroms. This material is available free of charge via the Internet at <http://pubs.acs.org>.

## References and Notes

- (1) Sandrone, G.; Dixon, D. A.; Hay, B. P. *J. Phys. Chem.*, submitted.
- (2) (a) Stern, P. S.; Chorev, M.; Goodman, M.; Hagler, A. T. *Biopolymers* **1983**, *22*, 1885. (b) Stern, P. S.; Chorev, M.; Goodman, M.; Hagler, A. T. *Biopolymers* **1983**, *22*, 1901.
- (3) Novoa, J. J.; Whangbo, M.-H. *J. Am. Chem. Soc.* **1991**, *113*, 9017.
- (4) Dauber-Osguthorpe, P.; Campbell, M. M.; Osguthorpe, D. J. *Int. J. Peptide Protein Res.* **1991**, *38*, 357.
- (5) (a) Aleman, C.; Perez, J. J. *J. Mol. Struct. (THEOCHEM)* **1993**, *285*, 221. (b) Aleman, C.; Perez, J. J. *Int. J. Peptide Protein Res.* **1993**, *41*, 606. (c) Aleman, C.; Puiggali, J. *J. Org. Chem.* **1995**, *60*, 910.
- (6) Aleman, C.; Perez, J. J. *Int. J. Peptide Protein Res.* **1994**, *43*, 258.
- (7) Tereshko, V.; Navarro, E.; Puiggali, J.; Subirana, J. A. *Macromolecules* **1993**, *26*, 7024.
- (8) Navarro, E.; Tereshko, V.; Subirana, J. A.; Puiggali, J. *Biopolymers* **1995**, *36*, 711.
- (9) Puiggali, J.; Munoz-Guerra, G. *J. Polym. Sci., Polym. Phys. Ed.* **1987**, *25*, 513.
- (10) Paiaro, G.; Pandolfo, L.; Busico, V.; Corradini, P. *Eur. Polym. J.* **1988**, *24*, 99.

- (11) Chan, G. Y. S.; Drew, M. G. B.; Hudson, M. J.; Iverson, P. B.; Liffenzin, J. O.; Skalberg, M.; Spjuth, L.; Madic, C. *J. Chem. Soc., Dalton Trans.* **1997**, 649.
- (12) Clement, O.; Rapko, B. M.; Hay, B. P. *Coord. Chem. Rev.* **1998**, *170*, 203.
- (13) Hay, B. P.; Clement, O.; Sandrone, G.; Dixon, D. A. *Inorg. Chem.* **1998**, *37*, 5887.
- (14) (a) Andzelm, J.; Wimmer, E.; Salahub, D. R. In *The Challenge of d and f Electrons: Theory and Computation*; Salahub, D. R., Zerner, M. C., Eds.; ACS Symposium Series 394; American Chemical Society: Washington, DC, 1989; p 228. (b) Andzelm, J. In *Density Functional Theory in Chemistry*; Labanowski, J., Andzelm, J., Eds.; Springer-Verlag: New York, 1991; p 155. (c) Andzelm, J. W.; Wimmer, E. *J. Chem. Phys.* **1992**, *96*, 1280. DGAUSS is a density functional program which is part of Unichem and is available from Oxford Molecular.
- (15) Godbout, N.; Salahub, D. R.; Andzelm, J.; Wimmer, E. *Can. J. Chem.* **1992**, *70*, 560.
- (16) Vosko, S. J.; Wilk, L.; Nusair, W. *Can. J. Phys.* **1980**, *58*, 1200.
- (17) (a) Becke, A. D. *Phys. Rev. A* **1988**, *38*, 3098. (b) Becke, A. D. In *The Challenge of d and f Electrons: Theory and Computation*; Salahub, D. R., Zerner, M. C., Eds.; ACS Symposium Series 394; American Chemical Society: Washington, DC, 1989; p 166. (c) Becke, A. D. *Int. J. Quantum Chem. Symp.* **1989**, *23*, 599.
- (18) Perdew, J. P. *Phys. Rev. B* **1986**, *33*, 8822.
- (19) Frisch, M. J.; Trucks, G. W.; Schlegel, H. B.; Gill, P. M. W.; Johnson, B. G.; Robb, M. A.; Cheeseman, J. R.; Keith, T. A.; Petersson, G. A.; Montgomery, J. A.; Raghavachari, K.; Al-Laham, M. A.; Zakrzewski, V. G.; Ortiz, J. V.; Foresman, J. B.; Cioslowski, J.; Stefanov, B. B.; Nanayakkara, A.; Challacombe, M.; Peng, C. Y.; Ayala, P. Y.; Chen, W.; Wong, M. W.; Andres, J. L.; Replogle, E. S.; Gomperts, R.; Martin, R. L.; Fox, D. J.; Binkley, J. S.; Defrees, D. J.; Baker, J.; Stewart, J. J. P.; Head-Gordon, M.; Gonzalez, C.; and Pople, J. A. Gaussian 94, revision E.2; Gaussian, Inc.: Pittsburgh, PA, 1995.
- (20) Bernholdt, D. E.; Apra, E.; Fruchtl, H. A.; Guest, M. F.; Harrison, R. J.; Kendall, R. A.; Kutteh, R. A.; Long, X.; Nicholas, J. B.; Nichols, J. A.; Taylor, H. L.; Wong, A. T.; Fann, G. I.; Littlefield, R. J.; Nieplocha, J. Parallel Computational Chemistry Made Easier: The Development of NWChem. *Int. J. Quantum Chem. Symp.* **1995**, *29*, 475.
- (21) (a) Dunning, T. H., Jr. *J. Chem. Phys.* **1970**, *53*, 2823. (b) Dunning, T. H., Jr.; Hay, P. J. *Methods of Electronic Structure Theory*; Plenum Press: New York, 1977.
- (22) Dunning, T. H., Jr. *J. Chem. Phys.* **1989**, *90*, 1007.
- (23) Kendall, R. A.; Dunning, T. H., Jr.; Harrison, R. J. *J. Chem. Phys.* **1992**, *96*, 6769.
- (24) (a) Steiner, T.; Saenger, W. *J. Am. Chem. Soc.* **1992**, *114*, 10146. (b) Steiner, T.; Saenger, W. *J. Am. Chem. Soc.* **1993**, *115*, 4540. (c) Tzuzuki, S.; Uchimaru, T.; Tanabe, K.; Hirano, T. *J. Phys. Chem.* **1993**, *97*, 1346. (d) Smith, G. D.; Jaffe, R. L.; Yoon, D. Y. *Chem. Phys. Lett.* **1998**, *289*, 480. (e) Novoa, J. J.; Lafuente, P.; Mota, F. *Chem. Phys. Lett.* **1998**, *290*, 519.
- (25) Kim, K.; Friesner, R. A. *J. Am. Chem. Soc.* **1997**, *119*, 12952.
- (26) Dixon, D. A.; Dobbs, K. D.; Valentini, J. J. *J. Am. Chem. Soc.* **1994**, *98*, 13435.
- (27) Torii, H.; Tatsumi, T.; Kanazawa, T.; Tatsumi, M. *J. Phys. Chem B* **1998**, *102*, 309.
- (28) (a) Schnur, D. M.; Yuh, Y. H.; Dalton, D. R. *J. Org. Chem.* **1989**, *54*, 3779. (b) Lii, J.-H.; Allinger, N. L. *J. Comput. Chem.* **1991**, *12*, 186.
- (29) Jorgensen, W. L.; Gao, J. *J. Am. Chem. Soc.* **1988**, *110*, 4212.
- (30) Herhe, W. J. *Practical Strategies for Electronic Structure Calculations*; Wavefunctions, Inc.: Irvine, CA, 1995.
- (31) (a) Sim, F.; Amant, St. A.; Papai, I.; Salahub, D. R. *J. Am. Chem. Soc.* **1992**, *114*, 4391. (b) Hill, R. A.; Labanowski, J. K.; Heisterberg, D. J.; Miller, D. D. In *Density Functional Theory in Chemistry*; Labanowski, J., Andzelm, J., Eds.; Springer-Verlag: New York, 1991; p 357.
- (32) Halgren, T. A. *J. Comput. Chem.* **1996**, *17*, 520.